Alkali-Aggregate Reaction in the Causeway Bridge, Perth, Western Australia

A. Shayan and C.J. Lancucki
CSIRO, Division of Building Research
Melbourne, Australia

ABSTRACT

A 36-year-old bridge in Perth, Western Australia, has shown severe map-cracking due to alkali-aggregate reaction. The bridge was constructed using several imported and local cements, some high in alkali. The aggregates found in the concrete are metadolerite of fine and medium textures, gneissic granite, and quartzite. Whereas none of these aggregates show any sign of reaction in the uncracked portions of the bridge, all of them, except the coarser grain metadolerite, show reaction rims in the cracked portions. The white deposit forming the rims within the aggregate periphery and also filling some air voids is a partially crystalline hydrated Na-K-Ca-silicate similar to those described in the literature, and shows a 12.2 Å spacing in its X-ray diffraction pattern. This reaction product has been characterized using scanning electron microscopy, electron probe microanalysis, infrared spectroscopy, and differential thermal analysis.

INTRODUCTION

The Causeway Bridge in Perth, Western Australia, was built in 1949-51 with several imported and local cements, some of which were high in alkali content. The aggregate used was from a local quarry containing metadolerite dykes through a granite mass. Map-cracking was noted some 15 years ago in the structure; it has widened with time. Some cracked portions were subsequently treated with an epoxy resin, but the cracks opened up further, and at present it seems that they are continuing to spread. The map-cracking of the affected portions of the bridge (Fig. 1) is indicative of alkali-aggregate reaction (AAR). This paper reports on the investigation of the concrete from the Causeway Bridge in relation to AAR.

EXPERIMENTAL

Map-cracking is not a uniform feature in the bridge. In one affected abutment the most reacted and cracked concrete pour is just above the water level, whereas in another abutment the corresponding pour shows no sign of cracking, but those higher up may be cracked. Seven cores, 100 mm diameter x 300 mm long, were drilled from the cracked and the uncracked portions of different abutments. They were photographed before being sawn lengthwise to expose the interior. A small portion of the half-cores was broken to reveal the fracture surfaces of the aggregates and the surrounding mortar and the remainder was used for making thin sections and for other studies.

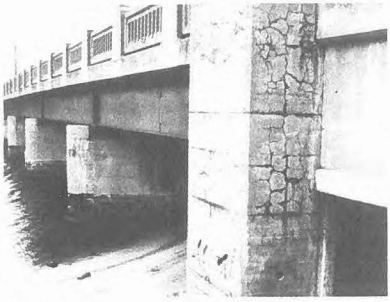

Fig.1. Map-cracking in an abutment of the bridge due to AAR.

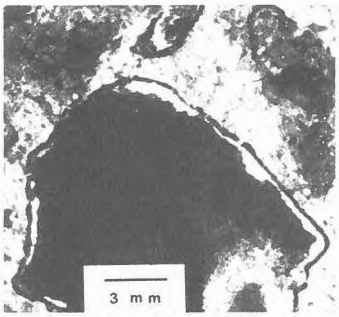

Fig.2. Reacted aggregate with black outer rim and white inner rim.

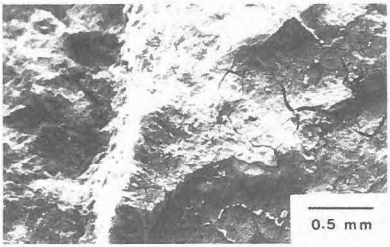

Fig.3. Gel with shrinkage cracks (right) around a reacted aggregate (left).

AAR reaction product found in aggregates as rims and in pores was removed for X-ray diffraction (XRD) analysis, infrared spectroscopy, scanning electron microscopy, electron probe microanalysis and for differential thermal analysis.

RESULTS

Cores drilled from uncracked portions showed no sign of reaction in the concrete; the aggregates were free of reaction rims and no reaction product was found within the aggregates, nor were any pores filled with the reaction product. The mortar surrounding the aggregates was also free of gel, and no microcracking was observed in the thin sections. The mortar contained a quartz sand, which showed no sign of reactivity with alkali. The aggregates in the concrete consisted of granitic, gneissic granite, and quartzitic rock types, in which strained quartz and fragmented feldspar crystals were present. A very fine grain and a fine to medium grain metadolerite, similar to those evaluated by Shayan et al. (1986), were also present in equal proportion to the other rock types.

Cores from cracked concrete showed all the symptoms of AAR. Strong reaction rims (Fig. 2) were obvious on the fracture surface of aggregates, forming a white deposit within the aggregate periphery. The corresponding surface of the mortar in the vicinity of such aggregates was covered with a gel which showed shrinkage cracking (Fig. 3). Some of the reacted aggregates showed internal cracking and some others were surrounded by gel-filled cracks extending into the mortar (Fig. 4). More severely cracked concretes showed more prominent white rims within the aggregate and more microcracking in the cement mortar. In addition to reaction rims, several filled pores were observed containing translucent or white material. These features have been observed in previously reported cases of AAR (Oberholster and Brandt 1976, Regourd et al. 1980, Cole et al. 1981, Grattan-Bellew 1981, Mather 1981, Buck 1983, Oberholster 1983, Fournier et al. 1985, and others).

Since the rock types in the reacted and unreacted concretes were the same, they must have had different reactivities with the different cements. This is an important case showing different behaviours of the same aggregates under different conditions, and the need for standard tests to take account of this factor and not rely on only one set of experimental conditions.

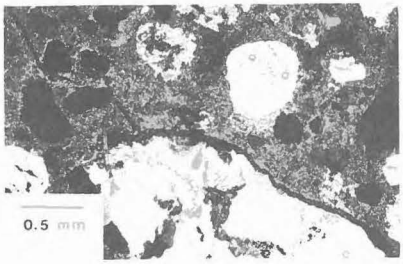

Fig.4. Gel-filled cracks around reacted aggregate and in the mortar. Crossed polarized light.

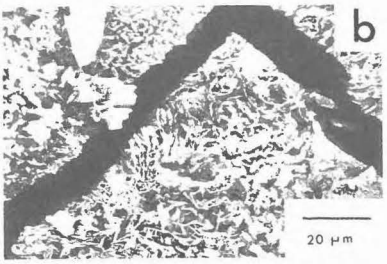

Fig.5. Portions of gel in Fig.3, partially (a) or fully (b) crystallized. Composition is largely Si and Ca with little K.

Characterization of reaction products

Microstructure: The gel shown in Fig. 3 was, in places, partially or fully crystallized (Fig.5) into plate-like crystals which energy dispersive X-ray spectroscopy (EDS) showed to contain Ca, Si and small amounts of K, similar to the gel observed by Regourd et al. (1981). It is uncertain whether the crystallization occurred within the concrete in situ or after the reacted concrete was exposed to the atmosphere. In some portions of the gel, small islands of ettringite (identified by XRD) were observed on the surface of the gel, but they do not appear to be associated with the AAR (Pettifer and Nixon 1981).

The micromorphology of the white reaction rim on the aggregates varied considerably depending on the type of aggregate. Generally, rims on gneissic granite and quartzite aggregates were thinner and showed much less crystallization (Fig. 6) than those on metadolerite aggregates (Fig.7). The regular rosettes of plate-like crystals (Cole et al. 1981, Regourd et al. 1981, Oberholster 1983, Fournier et al.1985) were only rarely observed on the reacted metadolerite aggregates. The material that had filled some pores was massive initially, but developed poorly crystalline features after exposure to the atmosphere. Some reaction rims appeared also to be a mixture of crystalline and amorphous material. Despite morphological differences, all these materials contained qualitatively similar amounts of Si, Ca, Na, and K, except the gel in Figs 3 and 5 which did not contain Na, and its K content was small.

Electron probe microanalysis (EPMA): An ARL Sem Q electron probe, in EDS mode, was used for quantitative EPMA (15 kV, 5 nA, 52.5° take off angle, and 100 s counting time). Table 1 gives the chemical composition of various reaction products. In view of the sensitivity of EPMA to the surface roughness of the materials from reaction rims (Figs 2, 6, and 7), these analyses may not be highly accurate. However, material from pore 1 which gave a strong 12.2 Å spacing (Fig. 8) was removed and pressed into a smooth flake to minimize surface roughness and then analysed. Materials in other pores were analysed in situ. These compositions, except for the Ca-rich material of pore 2, are less calcic than those of Cole and Lancucki (1983), but the sum of alkali oxides and CaO is nearly the same in some cases, or higher in other cases. The very low Na_2O contents reported by Oberholster (1983) may have arisen because of the high electron beam current (25 nA) that he employed; Na is unstable and evaporates under a high-current electron beam. Some of the analyses in Table 1 are similar to that reported by Mather (1981) when calculated on an ignited basis.

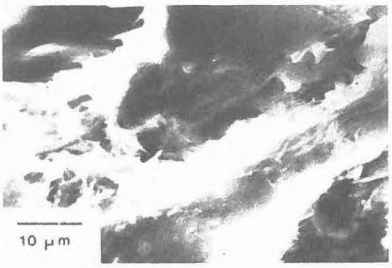

Fig.6. Massive AAR product (Si, Ca, K, Na) on a granitic aggregate.

Averaging all these analyses, excluding that for the Ca-rich phase, yields 68.2% SiO_2, 1.1% Al_2O_3, 12.5% CaO, 7.6% Na_2O, and 10.4% K_2O. Based on a structural formula with 46 oxygens, like that of okenite Ca_{10} Si_{18} $O_{46}.18H_2O$ (Merlino 1983) the average anhydrous analysis gives $Ca_{3.9}$ $Na_{4.3}$ $K_{3.9}$ $Si_{19.9}$ $Al_{0.36}$ O_{46} which has an excess of Si and other cations relative to okenite. Electron probe analysis of Poona okenite yielded $Ca_{9.7}$ $Si_{18.1}$ O_{46} which agrees well with the above formula for okenite. XRD analysis (see later) showed a small quartz impurity, and microanalytical measurement of H and C in an air-dried reaction product from a pore indicated 14.2% H_2O (cf. 16.5% H_2O in the okenite formula) and 4.5% $CaCO_3$, so that some of the excess cations in the average calculated formula could be due to impurities.

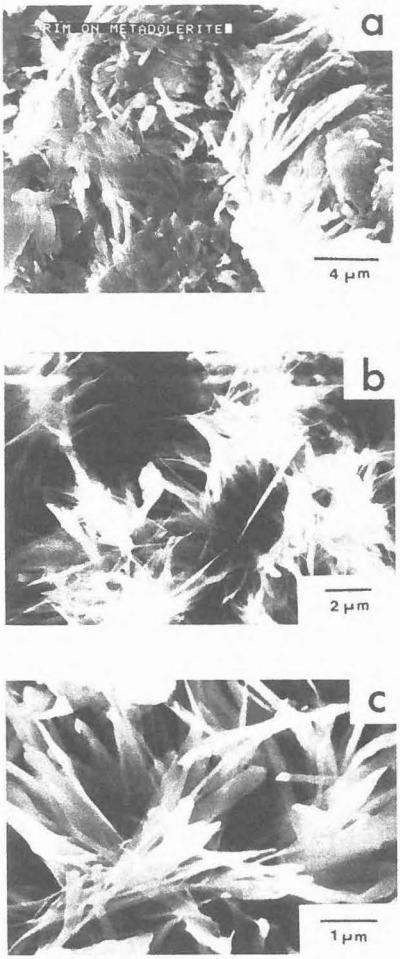

Fig.7. Various crystal habits from white reaction rim on metadolerite aggregates: (a) mixture of amorphous and crystalline material, (b) crystals not well formed, and (c) highly crystalline AAR products. All forms contain Si, Ca, Na, K.

X-ray diffraction study: Moist, soft, translucent materials from pores, exposed after cutting the cores, were used immediately for taking XRD patterns. Despite its gelatinous appearance, this type of material contained a well-crystallized component that gave the XRD pattern of Fig. 8 (B). Apart from minor differences this pattern is similar to that of the AAR products from a 24-year-old bridge (Buck and Mather 1978), from an Australian dam (Cole et al. 1981), and from the Landsdowne bridge in South Africa (Oberholster 1983). As shown in Fig.8 (C) and (D), this material is very unstable to heat, and the resulting loss of moisture was found to be largely irreversible. Therefore, differences in the state of hydration would result in differences in XRD patterns. Reaction product removed from the rim on the metadolerite aggregate (Fig. 2) resulted in a slightly different XRD pattern in that it contained a very weak 9.80 Å spacing and lacked the 10.09 and 8.54 Å spacings. A 9.55 Å and 9.70 Å has been observed by Cole et al. (1981) and Oberholster (1983) respectively, and could be due to a phase other than the 12.2 Å phase.

The 12.2 Å phase and that after heating at 110°C have been identified as precursor of okenite, and okenite, respectively (Cole and Lancucki 1983). The okenite pattern given in Fig. 8 (A) shows considerable differences from that of the heated AAR product (Fig. 8 (D)) reported here. The 4.26 Å and 3.34 Å spacings in these patterns could be due to a slight quartz impurity. Although the 3.05 Å spacing in Fig. 8 (B) is due largely to the 4th-order reflection of the 12.2 Å, the smaller 3.04 Å spacing in the XRD patterns of the heated samples is due to the carbonate impurity.

Infrared spectroscopy: The infrared spectra of the okenite and the AAR product from the bridge are given in Fig. 9. Absorption bands around 3400 cm^{-1} and 1650 cm^{-1} are due to water molecules, and that around 1400-1430 cm^{-1} due to carbonate molecules. Other absorption bands between 1000-1200 cm^{-1} are due to Si-O vibrations and the okenite spectrum (Fig.9(A)) shows a few absorption bands additional to that of the AAR product (Fig.9(B)) which is interpreted as being due to a more complex structure than the AAR product. The spectrum of the heated (210°C) AAR product (Fig.9(C)) shows that it is very unstable to heat as compared to the heated (310°C) okenite (Fig.9(D)). These observations are in agreement with the XRD data.

Thermal analysis: The differential thermal and thermogravimetric data for the AAR product in a pore (12.2 Å phase) are given in Fig. 10. The endotherms at 83, 94, and 164°C are due to loss of water. The small exotherm from 250-300°C may be due to oxidation of slight Fe impurities. The exotherm at 695°C is due to the recrystallization of a new phase which could not be identified from its XRD pattern, and the endotherm that occurred without any weight loss at 955°C is due to melt formation, where a clear glassy material had formed.

The thermal behaviour of this AAR product is also different from okenite (Phadke and Kshirsagar 1980), which lost water at 100, 190, and 370°C and showed an exotherm at about 900°C due to conversion to Wollastonite. The AAR product did not convert into Wollastonite.

TABLE 1 - Electron probe microanalysis of the reaction products

	White rim in Fig. 2 (6)*	White rim in Fig. 6 (10)	Pore 1 Pressed flake (10)	Pore 2 Ca-rich (3)	Pore 2 Si-rich (4)	Pore 3 (3)	Pore 4 (14)
SiO_2	65.6	64.0	71.0	43.8	70.4	64.0	67.4
Al_2O_3	1.0	1.8	0.1	1.7	0.8	1.6	1.2
FeO	0.7	0.9	<0.1	<0.1	<0.1	<0.1	0.4
MgO	0.5	0.9	<0.1	1.4	1.0	1.1	0.6
CaO	12.1	12.3	15.5	39.2	13.7	7.8	11.4
Na_2O	7.8	8.7	3.6	7.9	7.0	14.1	7.7
K_2O	11.9	10.7	9.7	5.0	6.9	10.3	11.0
SO_3	<0.1	0.6	0	0	0	0	0.2

*Number of analyses

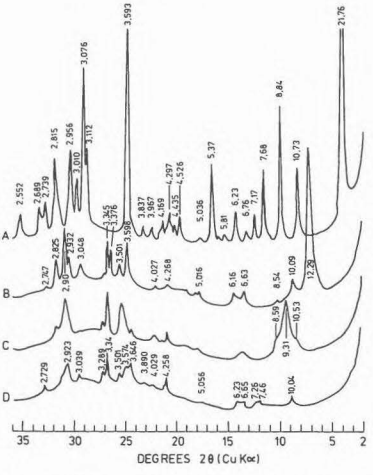

Fig.8. XRD patterns of (A) okenite from Poona, India, (B) unheated ARR product from pore 1 (Table 1), (C) material in (B) heated at 50°C for 3 hours and (D) material in (C) heated at 110°C for 2 hours.

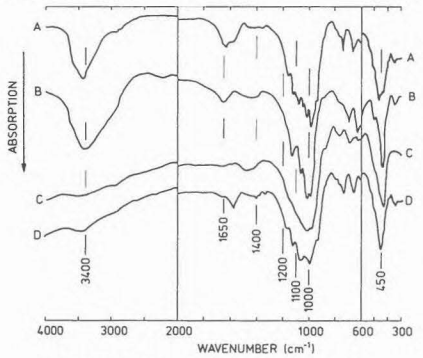

Fig.9. Infrared spectra of (A) unheated Poona okenite, (B) unheated AAR product from pore 1 (Table 1), (C) material in (B) heated at 210°C for 2 hour, and (D) Poona okenite heated at 310°C for 4 hours.

CONCLUSIONS

Alkali-aggregate reaction has taken place in the Causeway Bridge in Perth, Western Australia, and, in view of the dimensional stability of the aggregates used, is the likely cause of the observed pattern cracking. All aggregate types in the bridge had reacted in the cracked portions where the cement alkali was presumably high, but none had reacted in the uncracked portions where the alkali level was presumably low. The reaction product is broadly similar to those of other reported cases of AAR. The product is unlike any documented mineral or compound and requires further work for its precise identification.

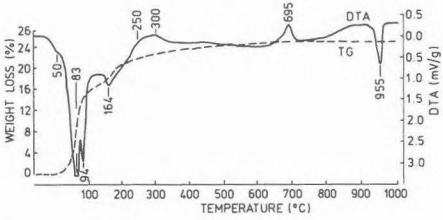

Fig.10. DTA and TG curves for AAR product from pore 1 (Table 1).

ACKNOWLEDGMENTS

The authors thank the Main Roads Department, Western Australia, for providing the concrete cores and Fig. 1, and Dr John Hamilton of the CSIRO Division of Mineral Chemistry for the thermal analysis.

REFERENCES

Buck, A.D. 1983. Cement Concrete and Aggregates, CCAGDP5: 131-133.

Buck, A.D., and Mather, K. 1978. In Proc. 4th Int. Conf. on the Effect of Alkalis in Cement and Concrete, Purdue University, 73-85.

Cole, W.F., and Lancucki, C.J. 1983. Cem. Conc. Res. 13:611-618.

Cole, W.F., Lancucki, C.J., and Sandy, M.J. 1981. Cem. Conc. Res. 11:443-454.

Fournier, B., Berube, M.A., and Vezina, D. 1985. Report GGL 85-32, Geology Department, Laval University, 40 pp.

Grattan-Bellew, P.E. 1981. In Proc. 5th Int. Conf. on Alkali-aggregate Reaction in Concrete, ed. R.E. Oberholster, Cape Town, S252/6, 11 p.

Mather, K. 1981. Cement Concrete and Aggregates, CCAGDP3: 53-62.

Merlino, S. 1983. Amer. Mineral 68:614-622.

Oberholster, R.E. 1983. In Proc. 6th Int. Conf. on Alkalis in Concrete, eds G.M. Idorn and S. Rostam, Copenhagen, 419-433.

Oberholster, R.E., and Brandt, M.P. 1976. In Proc. Symposium on the Effect of Alkali on the Properties of Concrete, London, 291-304.

Pettifer, K., and Nixon, P.J. 1981. Cem. Conc. Res. 11:801-802.

Phadke, A.V., and Kshirsagar, L.K. 1980. Mineral Mag. 43:677-679.

Regourd, M., Harnain, H., and Mortureux, B. 1980. Durability of Building Materials and Components, ASTM STP 691, eds P.J. Sereda and G.G. Litvan, 253-268.

Regourd, M., Hornain, H., and Poitevin, P. 1981. In Proc. 5th Int. Conf. on Alkali-aggregate Reaction in Concrete, ed. R.E. Oberholster, Cape Town, S252/35, 10 pp.

Shayan, A., Diggins, R., Ritchie, D.F., and Westgate, P. 1986. In Proc 7th Int. Conf. on Alkali-Aggregate Reaction, Ottawa (this volume).